MEASURING THE BIPOLAR CHARGE DISTRIBUTIONS OF FINE PARTICLE AEROSOL CLOUDS OF COMMERCIAL PMDI SUSPENSIONS USING A BIPOLAR NEXT GENERATION IMPACTOR (BP-NGI)

Martin Rowland[1,2*], Alessandro Cavecchi[3.4], Frank Thielmann[3], Janusz Kulon[5], Jag Shur[1] and Robert Price[1]

[1] Pharmaceutical Surface Science Research Group, Department of Pharmacy and Pharmacology, University of Bath, BA2 7AY, UK

[2] Pfizer Ltd, Discovery Park House, Sandwich, Kent, CT13 9NJ

[3] Novartis Pharma AG, Forum 1, Novartis Campus, CH 4056, Basel, Switzerland

[4] Chiesi Farmaceutici S.p.A, Via Palermo, 26 A, 43122, Parma, Italy.

[5] Faculty of Computing, Engineering and Science, University of South Wales, , CF37 1DL, UK

***Corresponding author:**

Dr Martin Rowland

Telephone: +44 (0) 1304 642508;

E-mail: Martin.Rowland@pfizer.com

ABSTRACT

Purpose: To measure the charge to mass (Q/M) ratios of the impactor stage masses (ISM) from commercial Flixotide™ 250 µg Evohaler, containing fluticasone propionate (FP), Serevent™ 25 µg Evohaler, containing salmeterol xinafoate (SX), and a combination Seretide™ 250/25 µg (FP/SX) Evohaler metered dose inhalers (MDIs). Measurements were performed with a purpose built bipolar charge measurement apparatus (bp-NGI) based on an electrostatic precipitator, which was directly connected below Stage 2 of a next generation impactor.

Methods: Five successive shots of the respective MDIs were actuated through the bp-NGI. The whole ISM doses were electrostatically precipitated to determine their negative, positive and net Q/m ratios.

Results: The ISM doses collected in the bp-NGI were shown to be equivalent to those collected in a standard NGI. FP particles, actuated from Flixotide™ and Seretide™ MDIs, exhibited greater quantities of negatively charged particles than positive. However, the Q/m ratios of the positively charged particles were greater in magnitude. SX particles from Serevent™ exhibited a greater quantity of positively charged particles whereas SX aerosol particles from Seretide™ exhibited a greater quantity of negatively charged particles. The Q/m ratio of the negatively charged SX particles in Serevent™ was greater in magnitude than the positively charged particles.

Conclusions: The bp-NGI was used to quantify the bipolar Q/m ratios of aerosol particles collected from the ISMs of commercial MDI products. The positive charge recorded for each of the three MDIs may have been enhanced by the presence of charged ice crystals formed from the propellant during the aerosolisation process.

KEY WORDS

Electrostatic charge

Bipolar charge

Pressurized metered dose inhaler

Bipolar next generation impactor

ABBREVIATIONS

API	Active pharmaceutical ingredient
BNC	Bayonet Neill-Concelman
BOLAR	Bipolar Charge Analyser
bp-NGI	Bipolar Next Generation Impactor
DC	Direct current
ED	Emitted dose
ELPI	Electrical low pressure impactor
ESPART	Electrical single particle aerodynamic relaxation time
FP	Fluticasone Propionate
HFA	Hydrofluroalkane
HPLC	High Performance Liquid Chromatography
ISM	Impactor stage mass
NGI	Next generation impactor
pMDI	Pressurized metered dose inhaler
RD	Recovered dose
SX	Salmeterol Xinafoate

INTRODUCTION

A metered dose inhaler (MDI) typically consists of a coated or uncoated aluminium can, a crimped metering valve containing a solution or suspension based formulation of an active pharmaceutical ingredient (API), held under pressure within a liquefied propellant such as HFA 134a or HFA 227. Formulations may also require the addition of a surfactant(s), to stabilise the dispersion of the API within the formulation (1). While in suspension, API particles come into contact with the inner walls of the canister, metering chamber and the components of the metering valve (elastomers, spring and stem) (2). For both HFA 134a and 227, the increased polarity compared to the original CFC propellants significantly increases the availability for the uptake of water. Thus, when formulating a suspension MDI the physical stability may be influenced by the amount of water in a formulation and the ingress rates of moisture via the metering valve.

The major factor that links the properties of the formulation to the respirable dose is the atomisation process. The actuation of an MDI, initiated by the depression of the valve stem, leads to the discharge of a metered volume via an expansion chamber. This process leads to high shear flow and flash evaporation of the liquefied propellant, created by the sudden decrease in pressure. The resultant droplets enter a highly kinetically energetic state, undergoing numerous collisions with each other and with the inner surfaces of the valve stem and the actuator orifice before being emitted from the actuator as a jet spray. During these collisions electron transfer may occur to or from the API particles via the mechanism of triboelectrification, causing the creation of highly charged species (3). Due to the multi-component nature of the system, the precise mechanisms remain relatively poorly understood; although it has been hypothesised that charge transfer may occur as a result of differences in the electrical properties of the materials involved. The canister and spring are generally constructed of conductive metals, although the inner surfaces of the aluminium cans can be coated with a low surface free energy polymer, whereas the valve, valve seals, stem are generally made from insulating plastics. The API

particles, which are electrically resistive, may also come into contact with the inner surfaces during which time charge transfer may occur. The amount of charge transferred will depend on the difference between the effective work functions of the two materials coming into contact, which is a measure of how much energy is required to remove an electron from the Fermi level of the material to the vacuum energy level (4). Charge transfer ceases when the Fermi levels of the two materials become equal, minimising the energy difference (5). In addition, as the HFA transitions into the vapour phase, rapid evaporative cooling will occur which may result in any soluble water present forming solid ice crystals which may also carry a charge (6).

As a result of these complex surface interactions experienced between the pMDI formulation and device components, aerosolised drug particles emitted may become both negatively and positively charged, resulting in a bipolar charge distribution, which may be difficult to accurately measure using conventional net charge measurement methods.

Various attempts have been made to accurately quantify the charge build up on aerosol particles in proportion to their mass. Ali *et al*. utilised an electrical single particle aerodynamic relaxation time (ESPART) analyser to determine electrodynamic effects of some sample DPI and pMDI formulations (7). Although the system provides measurements of bipolar charge-to-mass ratio, only single particle measurements may be recorded and not the entire deposited aerosol dose per shot. In addition, the ESPART measures charge and particle size by the particle number and not by mass or volume. Conversion of the distributions from a number based system may introduce error and so the data from the ESPART may be of limited relevance for pharmaceutical aerosols. The first widely available commercial method developed was the ELPI (electrical low pressure impactor) in which a Berner-type multi-jet low pressure impactor was modified such that the impaction plates are electrically isolated and connected to electrometers allowing for simultaneous net charge measurements and mass quantifications to be performed (8). Glover and Chan used the ELPI to measure the net charge of both

Flixotide™ and Ventolin™ pMDIs (9). For Flixotide™, they found that at higher particle cut off diameter, an overall net negative charge was recorded. At lower particle cut off diameter, an overall net positive charge was recorded. When plotted against the mass of deposited fluticasone propionate (FP) particles, at the lower cut off diameters, almost no FP was deposited, but a large net positive charge was recorded. This may be due to the presence of water which forms ice crystals during the actuation of the pMDI, the mass of which cannot be determined by conventional chromatographic methods (6). The study was further expanded to include Intal™, Tilade™ and QVAR™ pMDIs together with Flixotide™ and Ventolin™ (10).

The principles governing the mode of operation of the ELPI were used in the development of the Electrical Next Generation Impactor (eNGI), in which insulated NGI impaction cups are connected to an electrometer and the net charge-to-mass ratios of aerosol particles determined (11). The eNGI was successfully used to determine the effect of flow rate on the net charge-to-mass ratios of the Fine Particle Fraction (FPF) of Flixotide and Seretide pMDIs (12). Both the ELPI and eNGI allow the mass of the aerosol particles to be quantified but do not take into account the bipolar nature of the aerosol particles, providing only a measurement of the net electrostatic charge.

By utilising electrostatic precipitation, positively and negatively charged aerosol particles may be separated by means of an electric field generated by a high voltage source (13). Early systems such as those developed by O'Leary *et al*. and Kulon *et al*. allowed for the bipolar charge-to-mass ratios of aerosol particles to be measured (14, 15). However, these systems were not ideally suitable for performing accurate quantification of the amount of aerosol particles deposited and as such did not allow accurate measurement of bipolar charge-to-mass ratios to be performed.

More recently Dekati Ltd. have developed a novel instrument for measuring the electrostatic charge of aerosol particles called the BOLAR™. The instrument is designed such that the principal of electrostatic

precipitation is combined with an aerodynamic particle size classification system which allows for the bipolar charge-to-mass ratios of five different size fractions to be determined (16). Wong et al. used the system to measure the bipolar charge-to-mass ratios of spray dried mannitol particles from an Osmohaler® at flow rates of 30 and 60 L/min (17). The same authors then used modified Aerolizer™ devices to investigate the effect of inhaler design and inhaler material on the bipolar charge-to-mass ratios of spray dried mannitol particles (18). The BOLAR™ system was further used by Leung et al. to determine the bipolar charge-to-mass ratios of five particle size ranges for Intal Forte®, Tilade®, Ventolin® and QVAR® pMDIs at a flow rate of 60 L/min. The data showed QVAR® pMDI, which is a solution formulation, produced aerosol particles with a significantly different bipolar charge to mass distribution than the three other suspension type pMDIs (19). The authors further utilised the BOLAR™ to assess the use of a spacer on the bipolar charge-to-mass ratios of Tilade® pMDI. Interestingly, while the magnitude of the charge present on the positively charged respirable particles remained similar, the magnitude of the charge of the negatively charged particles was shown to decrease, along with the fine particle dose (20).

The present study introduces an additional tool to classify the bipolar charge-to-mass ratios of respirable aerosol particles. The set up consists of a modified Next Generation Impactor (NGI) which is an industry standard aerosol particle size classifier used to determine the *in vitro* performance of inhalable drug products (21). An electrostatic precipitation system is connected to a stage 2 of the NGI to allow measurement of the charge-to-mass ratio of the impactor stage mass (ISM). In addition, the complete emitted dose (ED) was recovered from the system in order to maintain accurate determination of the inhaler performance as would be determined by a normal NGI which has not been possible with other bipolar charge measurement systems previously developed. This bipolar Next Generation Impactor (bp-NGI) has been successfully used to characterise the bipolar charge to mass distributions of Flixotide™ 250, Serevent™ 25 and Seretide™ 250 pMDIs.

MATERIALS AND METHODS

Materials

Flixotide™ 250, Serevent™ 25, Seretide™ 250/25 Evohalers are suspension based pressurised metered dose inhaler (pMDI) formulations delivering 250µg of fluticasone propionate (FP), 25 µg salmeterol xinafaote (SX) and a combination of 250µg FP and 25 µg SX per actuation, respectively. These formulations contain the APIs suspended in HFA 134a propellant and were manufactured by GlaxoSmithKline (Ware, UK). Commercial samples of the pMDIs were supplied by AAH Pharmaceuticals Ltd. (Coventry, UK). Fluticasone propionate was supplied by Chemagis Ltd (Bnei Brak, Israel) and salmeterol xinafoate supplied by Neutech Laboratories (Hyderabad, India). All solvents used were of HPLC grade (Sigma-Aldrich, St. Louis, MO, USA). Ultra pure water was produced by reverse osmosis (MilliQ, Millipore, Molsheim, France). Ammonium acetate was purchased from Sigma Life Sciences (St. Louis, MO, USA).

Methods

Quantification of pMDI performance using the Next Generation Impactor (NGI)

The performance of the pMDIs was determined using a conventional NGI at 30 L/min (21). Five shots were actuated through the system. The APIs were recovered from the MDI actuator, mouthpiece and throat and collection cups. For stages 1-5 of the NGI the collection cups were washed with 20 mL of mobile phase, cups for stages 6-7 were filled with 5 mL of mobile phase and the cup for the MOC was filled with 10 mL of mobile phase to recover the API. Chemical analysis of the concentrations of the APIs was analysed using HPLC.

Design of the bipolar Next Generation Impactor (bp-NGI)

A schematic representation of a modified next generation impactor (NGI), incorporating two electrostatic precipitators for the collection of charged aerosols from any number of stages of an NGI (stage 2 through to stage 7) is shown in Figure 1. The modified system is known as the bipolar next generation impactor (bp-NGI). The bp-NGI was designed to collect and measure the charge-to-mass ratios of negatively and positively charged aerosol particles below a well-defined cut-off aerodynamic diameter.

In this study, the electrostatic precipitators were attached to stage 2 of the NGI, with a cut-off diameter of 6.40 µm at a flow rate of 30 L/min. The flow rate was controlled by a flow controller (TPK, Copley Instruments, Nottingham, UK) attached to a vacuum pump which was connected to the base of the electrostatic precipitators. Below the collection cup of stage 2, the aerosol dose is bifurcated into the two precipitators with an airflow rate of 15 L/min being pulled through each section. Each precipitator contained an earthed outer tube, to create a Faraday shield, a precipitation tube, a filter holder and a high voltage electrode, which was centrally positioned within the precipitation tube.

The bp-NGI was also designed to maintain laminar flow through the precipitators. The critical dimensions of the two electrostatic precipitators were designed to maximise the collection efficiency (K_{precip}) of the electrically mobile aerosol particles by adapting methodology used by Kulon et al. (22). The collection efficiency was determined using Equation 1.

$$K_{precip}\ (\%) = \frac{2}{r_2}\sqrt{\frac{Z_p V L}{v_o \ln(r_2/r_1)}} \times 100 \qquad \text{Equation 1}$$

Where Z_p is the electrical mobility of the charged aerosol particle, V is the voltage on the central electrode, L is the length of the electrode, v_o is the airflow rate, r_1 is the radius of the electrode and r_2 is the radius of the precipitation tube.

The calculated collection efficiencies of the bp-NGI at ±3.0 kV are shown in Figure 2 for aerosol particles exhibiting different amount of electrical charge at the cut-off diameters of the NGI stages at 30 L/min. Electrical mobilities of the particles were calculated according to Equation 2.

$$Zp = \frac{ne}{6\pi\eta_{air}r_p} \qquad \text{Equation 2}$$

Where n is the number of elementary charges on the particle, e is the elementary charge, 1.602 x 10^{-19} C, η_{air} is the viscosity of air at 25 °C, and r_p is the radius of the particle. The density of the particles was assumed to be 1 g/cm^3. The theoretical calculations suggested that particles below 6.40μm in diameter will be reasonably efficiently collected at ±3.0 kV, with a near maximum collection efficiency occurring when a particle gains a negative or positive charge equivalent to 200 electron charges per particle.

Methodology for Performing Bipolar Charge to Mass Measurements of Respirable Drug Particles Using the bp-NGI

Opposite polarity high DC voltage sources (Spellman, CZE1000R, West Sussex, UK) were connected to the electrically insulated copper electrodes, centrally located in the respective precipitators. A -3 kV voltage was applied to the negative electrode and a +3 kV to the positive electrode throughout this study. Aerosol particles with low electrical mobility, which cannot be precipitated onto either the electrodes or the precipitation tubes, were collected onto 0.45 μm pore size glass fibre filters (Whatman, Fisher Scientific, UK), housed at the base of each precipitation tube. The system is modular, such that each section of the apparatus can be isolated and separately washed down for drug quantification via HPLC.

During operation, the precipitation tubes were connected to a Keithley Instruments 6521 multi-input scanner card (Keithley Instruments, Reading, UK) connected to a Keithley 6517B electrometer for charge measurements. For each actuation of the inhaler device into the bp-NGI, the current versus time (I vs t profiles) profiles during aerosol deposition onto the two precipitation tubes were recorded and subsequently integrated to measure the positive and negative charge collected per shot. The cumulative amount of positive and negative charge for a well-defined number of shots was also measured. These values were divided by the total mass of drug collected within the positive and negative precipitation tubes to determine the net charge-to-mass ratio of the negatively and positively charged aerosols. During all experiments, the operator was connected to earth via a wrist band and the outer tubes surrounding the electrostatic precipitators were earthed to shield the precipitation tubes from stray external fields. During each experiment, a total of five shots of Flixotide™ 250, Seretide™ 250 and Serevent™ 25 were fired through the bp-NGI. The mass of the negatively, positively and neutrally charged particles was quantified via HPLC to calculate the bipolar charge to mass distribution within the bp-NGI. The experiments were performed in triplicate for statistical robustness. The temperature range for all experiments was 20°C ± 1 and the humidity range was 40% ± 2.

During operation, the electric field created by the negative electrode repels the negatively charged aerosol particles onto the negative precipitation tube, while the positively charged aerosol particles are attracted onto the electrode. Conversely, negatively charged aerosol particles in the oppositely charged precipitator are deposited onto the positive electrode while the positively charge aerosols are repelled onto the positive precipitation tube. The amount of drug collected on the negative precipitation tube and positive electrode indicated the quantity of drug particles that have sufficient negative electrical mobility to be precipitated within the two precipitators. The quantity of drug collected on the positive precipitation tube and negative electrode indicated the quantity of drug particles that are positively charged. The mass of drug collected from the respective filters represent the amount of aerosol dose which has insufficient positive or negative electrical mobility to be precipitated.

HPLC Analysis of Fluticasone Propionate and Salmeterol Xinafoate

Determination of the mass distribution of fluticasone propionate (FP) and salmeterol xinafoate (SX) was adapted from a previously published HPLC method (23). The HPLC system consisted of a pump (Jasco PU-980, Jasco Corp., Japan) coupled to an autosampler (Jasco AS-950) and UV detector (Jasco UV-975) set at 228 nm for simultaneous determination of both APIs. Separation was performed using a BDS Hypersil Column, 250x4 mm (Thermo Scientific, Waltham, MA, USA) maintained at 40^0C using a column oven (Jasco CO-965). The mobile phase was a mixture of methanol–0.6% (*w/v*) aqueous ammonium acetate solution (75:25%, *v/v*), filtered through a 0.45 µm nylon membrane (Whatman International Ltd., Maidstone, UK) and degassed. The retention time for salmeterol was 4.4 minutes and for fluticasone propionate was 5.4 minutes. Quantification was carried out by an external standard method and linearity was checked between 0.5 and 50 µg/mL for each individual API.

Statistical analysis

Linear regression analysis was used for the assessment of HPLC calibration. Statistical analysis between different populations was carried out using one-way analysis of variance. Comparison of the mean values was performed by Tukey's pair-wise comparison. All statistical analyses were performed using GraphPad Prism software (GraphPad Software Inc, California, USA). Error bars in graphical representations of data show ± standard deviation (S.D.) in all cases.

RESULTS AND DISCUSSION

Flixotide™ 250 and Serevent™ 25 pMDI were first tested with a conventional NGI in order to determine their conventional *in vitro* performance and to provide a comparison with the performance of the bp-NGI. The bp-NGI apparatus was connected to Stage 2 of the NGI and for each of the pMDIs, the mass deposition profiles within the electrostatic precipitators and bipolar charge measurements of the APIs were measured at both 0 V and ±3 kV. These measurements were then used to calculate the charge-to-mass ratios of both the negatively and positively charge aerosols generated by each pMDI.

Comparison of Conventional NGI and bp-NGI performance

A summary of the emitted doses and impactor stages masses for each API (as a percentage of the recovered dose) from Flixotide™ and Serevent™ pMDIs, as determined with a conventional NGI and with the bp-NGI (with electrostatic precipitators set to 0 Volts) are summarised in Table i. For each pMDI the results from each performance indicator were comparable, indicating that the addition of the electrostatic precipitation system to the bp-NGI had not adversely affected its ability to classify pMDI *in vitro* performance.

Bipolar charge-to-mass ratio determination of Flixotide™ 250

The mass deposition profile of FP from a commercial Flixotide™ 250 pMDI on the various sections of a bp-NGI at 0 V and ±3 kV are shown in Figures 3A and 3B, respectively, and summarised in Table ii. These data are expressed in terms of the mean quantity of drug deposited on each of the precipitation tubes, electrodes and filters and the relative percentage of the total amount of drug entering each precipitation section. When no voltage was applied to the central electrodes of the bp-NGI, over 95% of

the dose was recovered on the filters. The minimal deposition of FP on the electrodes and precipitation tubes at 0 V suggested laminar flow was maintained within each section. At 0 V, there was no significant difference ($p > 0.05$) in the quantities of FP entering each precipitation section of the bp-NGI (150.0 ± 10.7 µg and 149.4 ± 6.8 µg), indicating efficient bifurcation of the aerosol dose.

Upon applying -3 kV and +3 kV to the central electrodes of the two precipitators, similar quantities of FP were recovered, with only a relatively small percentage of the dose being collected on the filter. The percentage of aerosol particles collected on the negative and positive filters at ± 3.0 kV was 13.0 ± 1.2% and 11.6 ± 1.6%, respectively. For the positive precipitator section (+3.0 kV), 64.7 ± 1.4% of the mass collected was recovered on the central electrode, with 23.8 ± 1.7% of the aerosol particles precipitating on the positive precipitation tube. For the negative precipitator section (-3.0 kV), 25.0 ± 3.2% of the mass was collected on the central electrode, with 62.0 ± 2.3% on the negative precipitation tube. The mass ratios of the negatively to positively charged particles on the positive and negative sections of the bp-NGI were an average of 2.6:1. These data suggest that FP particles undergo sufficient triboelectrification upon aerosolisation to be electrostatically precipitated. These data also suggest that the FP particles are bi-polar in nature with the greater amount of particles less than 6.40 µm being negatively charged.

Individual shot-by-shot charge measurements on the precipitation tubes (labelled negative and positive) and their net charge values at 0 V and ±3.0 kV are shown in Figure 4A and 4B, respectively. Measuring in current versus time mode at 0 V, each precipitation section acts as a flow through Faraday pail, operating in a similar fashion to a system utilised by Chow et al. (24). At 0 V, both sections exhibited a net positive charge (average +0.04 ± 0.00 nC), which is in agreement with the research findings of Peart et al., that showed unlike the majority of marketed pMDI products, GSK's US FP pMDI product (Flovent®) consistently produced a net positively charged aerosol cloud (25). Conversely, Hoe et al., who used an electrical Next Generation Impactor (eNGI) to measure the net charge of Flixotide™ and Seretide™ on individual stages at three different flow rates, found that the net charge-to-mass ratios for particles of FP and SX were slightly negative and close to zero on a pC/µg level (12). Kwok et al. used

a Faraday well and an ELPI to measure the net charge-to-mass ratios of a range of pMDIs, including Flixotide™ (10). The overall net charge of the entire dose of a Flixotide™ pMDI as measured with a Faraday well was also found to be net positive, whereas on the individual stages of the ELPI the net charge on the stages which retained significant amounts of FP were net negative. However, on the lower stages of the ELPI (approximately <0.6 µm), where there was minimal drug recovery or the recovery was below the limit of detection, there was a polarity change and a significant amount of net positive charge was recorded. Since the number of elementary charges per droplet is well below the Raleigh limit, the possible source of this charge was purported by Kwok et al. to be possibly due to the presence of non-volatile water in the MDI, which may precipitate as small ice crystals from an evaporating HFA droplet (26). The ingress of water has also been shown to affect charging of the fine particle dose in a HFA-134a pMDI by Kulphaisal et al., who showed that when the water content increased above 300ppm the net charge inverted from negative to positive (6).

Upon applying -3 kV and +3 kV DC voltage to the respective negative and positive electrodes, the mean charge of the negatively charged FP particles per shot was recorded as -0.36 ± 0.01 nC, and the mean charge of the positively charged FP particles per shot was +0.43 ± 0.01 nC. The polarity of the net charge of the fine particle cloud per shot was electropositive and calculated to be +0.07 ± 0.01 nC. The net charge measurements for the aerosol dose below ≤ 6.4 µm at both 0 V and ± 3 kV are in good agreement with the previous findings (10).

The bipolar charge to mass (Q/m) ratio of the negative and positive charges from a Flixotide™ 250 pMDI are shown in Figure 5. The Q/m ratios of the negatively and positively charged particles were -18.0 ± 2.8 pC/µg and +68.8 ± 5.6 pC/µg, respectively. Whilst these data suggest that the charge per unit mass of the positively charged FP particles were significantly larger in magnitude than the negatively charged particles, the bp-NGI measurements do not account for the possible charging effects of the excipients and from the precipitation of ice crystals.

Bipolar charge-to-mass ratio determination of Serevent™ 25

The mass deposition profile of SX from a commercial Serevent™ 25 pMDI on the various section of the bp-NGI at 0 V and ±3 kV are shown in Figures 6A and 6B, respectively, and are summarised in Table iii. At 0 V, over 88% of the particles were collected on the filters, with no significant differences in the quantities entering each precipitator and the drug collected on the glass filters ($p > 0.05$).

Applying ±3 kV potential to the central electrodes significantly reduced the deposition of SX on the filters ($p < 0.05$). The percentage of low electrical mobility particles recovered from the filters dropped to below 14%. For both precipitators, there was a significantly greater recovery of positively charged SX particles than negatively charged SX particles. The mass ratio of positively charged to negatively charged particles in both precipitators was approximately 3:1.

Shot-by-shot charge measurements from the outer precipitation tubes for five consecutive shots at 0 V and ±3 kV are shown in Figures 7A and 7B, respectively. With no voltage being applied, the net charge of the SX particles was low and slightly electropositive for both precipitators. These data are not in agreement with net fine particle dose charge measurements of Peart et al., who found, with the use of an aerosol sampling apparatus, the net charge of SX was electronegative (-80 pC) (25). Applying -3 kV and +3 kV DC voltage to the respective negative and positive electrodes, there was no significant differences in the mean charge per shot of the negatively and positively charged SX particles (Table iv) The charge to mass (Q/m) ratios of the negatively and positively charged particles were -106.2 ± 23.4 pC/µg and +43.7 ± 3.3 pC/µg, respectively, and the overall net charge-to-mass ratio was +3.7 ± 4.5 pC/µg as shown in Figure 8.

In a similar trend to the Flixotide study, the low precipitated mass of SX particles (negatively charged SX) exhibited a significantly higher Q/m ratio than the higher precipitated mass. It appears that this higher charge-to-mass ratio may not be due to the specific charges of the negative SX particles but may

relate to the additional contribution of the propellant and the precipitation of impurities such as water upon propellant vaporisation. Whilst there has been no published ELPI studies with a Serevent product, a highly electronegative charge signal in the lower stages (<0.6µm) of an ELPI for a predominately net positively charged salbutamol sulphate aerosol was found by Kwok et al. for the excipient-free Ventolin pMDI product (10).

Bipolar charge-to-mass ratio determination of Seretide™ 250

The mass deposition profile of FP and SX from a commercial Seretide™ 250 pMDI in the bp-NGI at 0 V and ±3 kV are shown in Figures 9 A-D respectively, and summarised in Tables iv a for FP and iv b for SX. At 0 V, the majority (> 85%) of the FP and SX particles are collected on the glass filters at the base of the precipitators. Upon applying high voltage (±3 kV), similar quantities of FP and SX were recovered from each precipitation section of the bp-NGI, indicating efficient bifurcation of the fine particle cloud within the system. The mass ratio of negatively to positively charged particles of precipitated FP was 2.6:1, which is similar to that obtained for the Flixotide™ product.

The ratio of negatively to positively charged SX particles by mass was 1.7:1. This was not in good agreement with the Serevent pMDI, which indicated a mass ratio of negatively to positively charged SX particles of 0.6:1. These data suggest that the presence of a relatively high dose of FP (10:1 dose ratio of FP:SX) may have a significant impact on the mass deposition profile of SX within the electrostatic precipitator. The different deposition profile of SX particles may suggest that SX, which is predominately positively charged, has an attractive tendency to the negatively charged FP particles which could alter its deposition profiles and its response to an electric field. Agglomerate formation of FP with SX has previously been reported on individual impactor stages for Seretide™ pMDI formulation by Raman spectroscopy (27).

The charge measurements of FP and SX collected per shot recorded at 0V and ±3 kV are shown in Figure 10 A and B, respectively. At 0V, the net charge measurement in each precipitation was low and positive. At ±3 kV, the average charge measured per shot for the negative and positive precipitators were -0.37 ± 0.01nC and +0.47 ± 0.01nC, respectively, with an average net charge per shot of +0.10 ± 0.01nC. These results are similar to the behaviour of Flixotide, with the fine particle dose being electropositive.

The bipolar charge-to-mass ratios of the precipitated FP and SX from a Seretide™ 250 pMDI are shown in Figure 11. The charge-to-mass ratios of the negatively and positively charged particles were -11.5 ± 0.5 pC/µg and +42.8 ± 4.6 pC/µg, respectively, with a net charge-to-mass ratio of +2.6 ± 0.4 pC/µg. These findings suggest that presence of salmeterol has little effect on the electrostatic precipitation properties, which was dominated by the charging behaviour of FP and the influence of excipients leading to the higher than expected positive charge-to-mass ratio values.

A summary of the percentage mass distributions recorded by the precipitation sections of the bp-NGI of the three drug products are summarised in Table v. For both Flixotide™ and Seretide™ products, the FP exhibited similar profiles with 62.0 ± 2.3% and 61.2 ± 4.5% negatively charged particles, 25.0 ± 3.2% and 24.8 ± 2.7% of positively charged particles and 13.0 ± 1.2% and 14.1 ± 2.0% non-precipitated dose, respectively. These data indicated the presence of SX in combination with FP had little effect on the electrostatic properties of FP. For SX, the precipitation profiles of SX from Seretide™ and Serevent™ were directly affected by the presence of FP. The percentage of negatively charged particles of SX increased over 2.5-fold within the combination Seretide™ drug product. This concomitantly led to a similar decrease in the amount of positively charged particles in the combination drug product.

CONCLUSIONS

The present study demonstrates that the bipolar Next Generation Impactor may be successfully used to quantify the bipolar charge-to-mass ratios of the ISM from commercial pMDI formulations whilst at the same time allowing for complete recovery of the emitted dose from the inhaler. More negatively charged particles were produced than positively charged from both Flixotide™ and Seretide™ although the charge-to-mass ratios of the positively charged particles were larger in magnitude than the negatively charged indicating the possibility of competing triboelectric charging mechanisms. In the case of Serevent™, the SX particles showed a propensity to become more positively charged than negatively charged, however, the charge-to-mass ratios of the negatively charged particles were significantly larger in magnitude. The difference in behaviour between the SX particles in Serevent™ and Seretide™ may be attributed to the presence of FP-SX aggregates in Seretide™ which are not present in Serevent™. The results of the study illustrate that the bp-NGI is an effective tool to quantify the bipolar charge-to-mass ratios of respirable aerosol particles produced by the three commercially available pMDIs.

Comparisons with data generated by Kwok et al. with the ELPI indicated that the positive charge values recorded may have been contributed to by the presence of ice crystals exiting the inhaler as the pMDI propellant evaporated (10). A control experiment is suggested to characterise a propellant only pMDI formulation; values for the propellant bipolar charge could be subtracted from the overall bipolar charge in order to determine the contribution of the API to the charge values. Unfortunately placebo pMDI canisters of Flixotide™, Serevent™ and Seretide™ are not commercially available and could not be analysed for this study.

Further studies suggested include measuring the bipolar charge distributions of other pMDI formulations such as QVAR® and Ventolin® with the bp-NGI and comparing the bipolar charge-to-mass ratio values recorded with net charge-to-mass ratio values published in the literature. Other variables such as flow rate, dosage strength, humidity and the type and colour of the polymer used to disperse a pMDI could also be investigated as well as the addition of a spacer device. The bipolar charge of only the combined fine particle fraction from the bp-NGI from stages 2 and below of the NGI were collected, additional

experiments could also be performed to connect the electrostatic precipitation system to the other stages in order to build up a more accurate picture of the relationship between aerosol particle charge and aerodynamic diameter cut off.

ACKNOWLEDGEMENTS

The authors would like to thank Novartis AG for funding and Paul Frith at the University of Bath Department of Mechanical Engineering for assistance with design and construction of the bp-NGI.

References

1. Murata S, Izumi T, Ito H. Effect of the moisture content in aerosol on the spray performance of Stmerin ® D hydrofluoroalkane preparations (2). Chem Pharm Bull (Tokyo). 2012;60(5):593-7.
2. James J, Davies M, Toon R, Jinks P, Roberts CJ. Particulate drug interactions with polymeric and elastomeric valve components in suspension formulations for metered dose inhalers. International Journal of Pharmaceutics. 2009;366(1–2):124-32.
3. Kwetkus BA. Particle Triboelectrification and its Use in the Electrostatic Separation Process. Particulate Science and Technology. 1998;16(1):55-68.
4. Lowell J. The role of material transfer in contact electrification. J Phys D. 1977;10:L233-L5.
5. Matsusaka S, Maruyama H, Matsuyama T, Ghadiri M. Triboelectric charging of powders: A review. Chemical Engineering Science. 2010;65(22):5781-807.
6. Kulphaisal P, Peart J, Byron P, editors. Influence of water on electrical properties in hydrofluoroalkane based metered dose inhalers. Respiratory Drug Delivery VIII; 2002; Raleigh, NC: Davis Horwood International.
7. Ali M, Mazumder MK, Martonen TB. Measurements of Electrodynamic Effects on the Deposition of MDI and DPI Aerosols in a Replica Cast of Human Oral-Pharyngeal-Laryngeal Airways. Journal of Aerosol Medicine and Pulmonary Drug Delivery. 2009;22(1):35-44.
8. Keskinen J, Pietarinen K, Lehtimaki M. Electrical low pressure impactor. J Aerosol Sci. 1992;23(4):353-60.
9. Glover W, Chan H-K. Electrostatic charge characterization of pharmaceutical aerosols using electrical low-pressure impaction (ELPI). Journal of aerosol science. 2004;35(6):755-64.
10. Kwok P, Glover W, Chan HK. Electrostatic Charge Characteristics of Aerosols Produced from Metered Dose Inhalers. Journal of Pharmaceutical Sciences. 2005;94(12):2789-99.
11. Hoe S, Young P, Chan H-K, Traini D. Introduction of the electrical next generation impactor (eNGI) and investigation of its capabilities for the study of pressurized metered dose inhalers. Pharmaceutical research. 2009;26(2):431-7.
12. Hoe S. The Influence of Flow Rate on the Aerosol Deposition Profile and ElectrostaticCharge of Single and Combination Metered Dose Inhalers. Pharmaceutical research. 2009;26(12):2639.
13. Mizuno A. Electrostatic precipitation. IEEE Trans Dielectr Electr Insul. 2000;7(5):615-24.
14. O'Leary M, Balachandran W, Rogueda P, Chambers F. The bipolar nature of charge resident on supposedly unipolar aerosols. Journal of Physics: Conference Series. 2008;142:012022.
15. Kulon J, Balachandran W. The measurement of bipolar charge on aerosols. Journal of Electrostatics. 2001;51-52(0):552-7.
16. Yli-Ojanpera J, Ukkonen A, Jarvinen A, Layzell S, Niemela V, Keskinen J. Bipolar Charge Analyzer (BOLAR): A new aerosol instrument for bipolar charge measurements. J Aerosol Sci. 2014;77:16-30.
17. Wong J, Lin Y-W, Kwok PCL, Niemela V, Crapper J, Chan H-K. Measuring Bipolar Charge and Mass Distributions of Powder Aerosols by a Novel Tool (BOLAR). Mol Pharmaceutics. 2015;12(9):3433-40.

18. Wong J, Kwok PCL, Niemela V, Heng D, Crapper J, Chan H-K. Bipolar electrostatic charge and mass distributions of powder aerosols - Effects of inhaler design and inhaler material. J Aerosol Sci. 2016;95:104-17.
19. Leung SSY, Chiow ACM, Ukkonen A, Chan H-K. Applicability of Bipolar Charge Analyzer (BOLAR) in Characterizing the Bipolar Electrostatic Charge Profile of Commercial Metered Dose Inhalers (MDIs). Pharm Res. 2016;33(2):283-91.
20. Leung SSY, Chiow ACM, Kwok PCL, Ukkonen A, Chan H-K. Effect of Spacers on the Bipolar Electrostatic Charge Properties of Metered Dose Inhaler Aerosols-A Case Study With Tilade. J Pharm Sci. 2017;106(6):1553-9.
21. Marple VA, Roberts DL, Romay FJ, Miller NC, Truman KG, Van Oort M, et al. Next generation pharmaceutical impactor (a new impactor for pharmaceutical inhaler testing). Part I: Design. Journal of Aerosol Medicine. 2003;16(3):283–99.
22. Kulon J, Hrabar S, Machowski W, Balachandran W. A Bipolar Charge Measurement System for Aerosol Characterization. IEEE Transactions on Industry Applications. 2001;37(2):472-9.
23. Murnane D, Martin GP, Marriott C. Validation of a reverse-phase high performance liquid chromatographic method for concurrent assay of a weak base (salmeterol xinafoate) and a pharmacologically active steroid (fluticasone propionate). Journal of Pharmaceutical and Biomedical Analysis. 2006;40:1149–54.
24. Chow KT, Zhu K, Tan RBH, Heng PWS. Investigation of Electrostatic Behavior of a Lactose Carrier for Dry Powder Inhalers. Pharmaceutical Research. 2008;25(12):2822-34.
25. Peart J, Kulphaisal P, Orban JC. Relevance of Electrostatics in Respiratory Drug Delivery. Business Briefing: Pharmagenerics. 2003:1-4.
26. Kwok P, Noakes T, Chan H-K. Effect of moisture on the electrostatic charge properties of metered dose inhaler aerosols. Journal of aerosol science. 2008;39(3):211-26.
27. Theophilus A, Moore A, Prime D, Rossomanno S, Whitcher B, Chrystyn H. Co-deposition of salmeterol and fluticasone propionate by a combination inhaler. Int J Pharm. 2006;313(1-2):14-22.

Table and Figure Legends

Table i: Comparison of Flixotide™ 250 and Serevent™ 25 pMDI performance as determined with a conventional NGI and the bp-NGI.

Table ii: Mass and percentage mass of FP particles collected from each section of the bp-NGI precipitation system from 5 shots Flixotide™ 250 (n=3, mean ± SD) at A, 0 V and B ±3 kV.

Table iii: Mass and percentage mass SX particles collected from each section of the bp-NGI

precipitation system from 5 shots of Serevent™ 25 (n=3, mean ± SD) at A, 0 V and B ±3 kV.

Table iv: Mass and percentage mass of a, FP and b, SX particles collected from each section of bp-NGI precipitation system from 5 shots of a combination Seretide™ formulation (n=3, mean ± SD) at A, 0 V and B ±3 kV.

Table v: Percentages of negatively charged, positively charged and uncharged Particles of FP and SX in Flixotide™, Seretide™ and Serevent™ pMDIs ± SD, n=3.

Figure 1: Design of the BP-NGI

Figure 2: Theoretical collection efficiency of bp-NGI plotted against particle diameter cut off diameter of NGI stages 1-8 for 100, 200 and 300 electrons per particle.

Figure 3: Percentage mass of FP particles collected from each section of bp-NGI precipitation system from 5 shots of Flixotide™ 250 (n=3, mean ± SD) at A, 0 Volts and B ±3000 Volts.

Figure 4: Charge measurements of FP particles collected from each section of the bp-NGI precipitation system from 5 shots of Flixotide™ 250 (n=3, mean ± SD) at A, 0 Volts and B ±3000 Volts.

Figure 5: Bipolar charge-to-mass ratios of FP particles from 5 shots of Flixotide™ 250 (n=3, mean ± SD).

Figure 6: Percentage mass of salmeterol particles collected from each section of bp-NGI precipitation system from 5 shots of Serevent™ 25 (n=3, mean ± SD) at A, 0 Volts and B ±3000 Volts.

Figure 7: Charge measurements of SX particles collected from each section of the bp-NGI precipitation system from 5 shots of Serevent™ 25 (n=3, mean ± SD) at A, 0 Volts and B ±3000 Volts.

Figure 8: Bipolar charge-to-mass ratios of SX particles from 5 shots of Serevent™ 25 (n=3, mean ± SD).

Figure 9: Percentage mass of FP particles collected at A, 0 Volts and B ±3000 Volts and percentage mass of salmeterol particles at C, 0 Volts and D ±3000 Volts collected from each section of bp-NGI precipitation system from 5 shots of Seretide™ 250 (n=3, mean ± SD).

Figure 10: Charge measurements of SX and FP particles collected from each section of the bp-NGI precipitation system from 5 shots of Seretide™ 250 (n=3, mean ± SD) at A, 0 Volts and B ±3000 Volts.

Figure 11: Bipolar charge-to-mass ratios of SX and FP particles from 5 shots of Seretide™ 250 (n=3, mean ± SD).

Tables

Table i.

pMDI	Conventional NGI		bp-NGI	
	ED (% of RD)	ISM (% of RD)	ED (% of RD)	ISM (% of RD)
Flixotide™ 250	89.8 ± 4.0	50.2 ± 2.6	91.0 ± 6.0	49.8 ± 5.7
Serevent™ 25	88.5 ± 4.8	58.3 ± 3.6	91.5 ± 11.6	64.1 ± 9.0

Table ii.

FP

	0 V				±3 kV			
	Negative Precipitator (µg ± SD)	Positive Precipitator (µg ± SD)	Negative Precipitator (% ± SD)	Positive Precipitator (% ± SD)	Negative Precipitator (µg ± SD)	Positive Precipitator (µg ± SD)	Negative Precipitator (% ± SD)	Positive Precipitator (% ± SD)
Tube	2.8 ± 0.3	0.6 ± 0.3	1.9 ± 0.2	0.4 ± 0.2	95.2 ± 3.6	35.0 ± 2.5	62.0 ± 2.3	23.8 ± 1.7
Electrode	8.3 ± 1.1	3.7 ± 1.1	5.5 ± 0.8	2.4 ± 0.7	38.4 ± 4.9	95.1 ± 2.0	25.0 ± 3.2	64.7 ± 1.4
Filter	139.0 ± 9.3	145.2 ± 2.3	92.7 ± 6.2	97.2 ± 5.2	19.9 ± 1.6	17.0 ± 2.3	13.0 ± 1.2	11.6 ± 1.6
Total	150.0 ± 10.7	149.4 ± 6.8	100.0 ± 7.1	100.0 ± 6.1	153.5 ± 10.0	147.0 ± 6.8	100.0 ± 6.6	100.00 ± 4.6

Table iii.

SX

	0 V				±3 kV			
	Negative Precipitator (µg ± SD)	Positive Precipitator (µg ± SD)	Negative Precipitator (% ± SD)	Positive Precipitator (% ± SD)	Negative Precipitator (µg ± SD)	Positive Precipitator (µg ± SD)	Negative Precipitator (% ± SD)	Positive Precipitator (% ± SD)
Tube	1.0 ± 0.5	0.6 ± 0.1	8.2 ± 3.8	5.1 ± 1.4	3.9 ± 0.4	10.8 ± 0.9	20.1 ± 2.29	58.9 ± 5.7
Electrode	0.5 ± 0.1	0.8 ± 0.2	4.2 ± 0.8	6.4 ± 1.8	10.1 ± 1.2	3.6 ± 0.9	65.7 ± 6.9	27.9 ± 5.5
Filter	10.3 ± 0.7	10.8 ± 0.5	87.6 ± 6.0	88.5 ± 3.8	2.4 ± 0.2	2.2 ± 0.1	14.2 ± 1.0	13.6 ± 0.7
Total	11.9 ± 1.3	12.2 ± 0.8	100.0 ± 10.6	100.0 ± 6.1	16.3 ± 1.8	16.5 ± 1.9	100.0 ± 10.2	100.0 ± 11.9

Table iva.

FP

	0 V				±3 kV			
	Negative Precipitator (µg ± SD)	Positive Precipitator (µg ± SD)	Negative Precipitator (% ± SD)	Positive Precipitator (% ± SD)	Negative Precipitator (µg ± SD)	Positive Precipitator (µg ± SD)	Negative Precipitator (% ± SD)	Positive Precipitator (% ± SD)
Tube	2.3 ± 0.7	6.9 ± 1.6	1.6 ± 0.5	4.4 ± 1.0	105.6 ± 7.8	40.7 ± 2.2	61.2 ± 4.5	23.5 ± 1.3
Electrode	6.1 ± 1.3	8.7 ± 2.9	4.3 ± 0.9	5.5 ± 1.9	42.8 ± 4.7	108.4 ± 7.8	24.7 ± 2.7	62.7 ± 4.5
Filter	133.8 ± 6.1	141.8 ± 7.7	94.1 ± 4.3	90.1 ± 4.9	24.4 ± 3.4	23.8 ± 3.1	14.1 ± 2.0	13.8 ± 1.8
Total	142.2 ± 8.0	157.4 ± 12.2	100.0 ± 5.6	100.0 ± 7.7	172.8 ± 15.8	172.9 ± 13.0	100.0 ± 9.2	100.0 ± 7.5

Table ivb.

SX

	0 V				±3 kV			
	Negative Precipitator (µg ± SD)	Positive Precipitator (µg ± SD)	Negative Precipitator (% ± SD)	Positive Precipitator (% ± SD)	Negative Precipitator (µg ± SD)	Positive Precipitator (µg ± SD)	Negative Precipitator (% ± SD)	Positive Precipitator (% ± SD)
Tube	0.7 ± 0.1	0.8 ± 0.2	5.4 ± 1.0	6.1 ± 1.4	6.7 ± 0.3	4.6 ± 0.4	52.8 ± 2.7	31.6 ± 2.7
Electrode	0.5 ± 0.1	1.1 ± 0.3	4.2 ± 1.0	8.2 ± 1.8	3.8 ± 0.3	7.4 ± 0.4	30.1 ± 2.2	51.2 ± 2.4
Filter	10.6 ± 0.7	11.0 ± 0.7	90.4 ± 5.4	85.7 ± 5.4	2.2 ± 0.4	2.5 ± 0.7	17.2 ± 2.9	17.2 ± 4.9
Total	11.8 ± 0.9	12.9 ± 1.1	100.0 ± 7.5	100.0 ± 8.6	12.6 ± 1.0	14.5 ± 1.5	100.0 ± 7.8	100.0 ± 10.0

Table v.

	FP		**SX**	
	Flixotide™	Seretide™	Seretide™	Serevent™
Negatively charged particles (% ± SD)	62.0 ± 2.3	61.2 ± 4.5	52.8 ± 2.7	20.1 ± 2.3
Positively charged particles (% ± SD)	25.0 ± 3.2	24.8 ± 2.7	30.1 ± 2.2	65.7 ± 6.9
Uncharged particles (% ± SD)	13.0 ± 1.2	14.1 ± 2.0	17.2 ± 2.9	14.2 ± 1.0

Figures

Figure 1

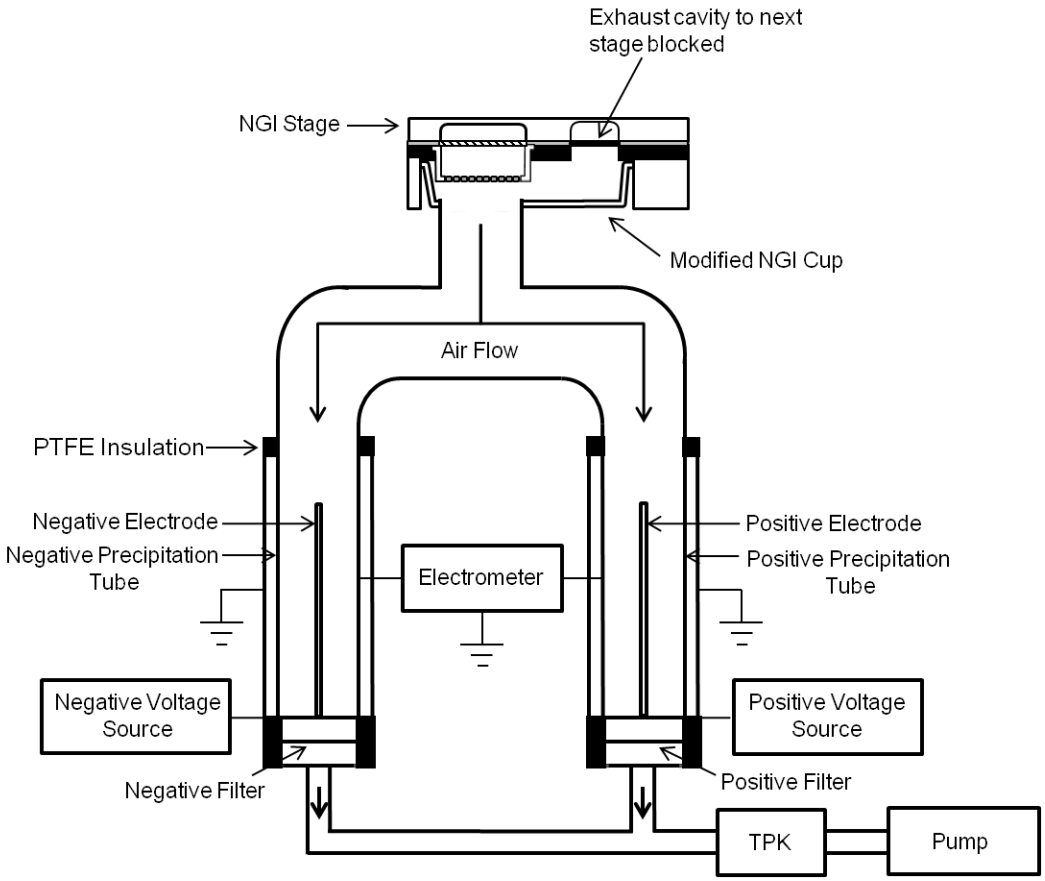

Figure 2

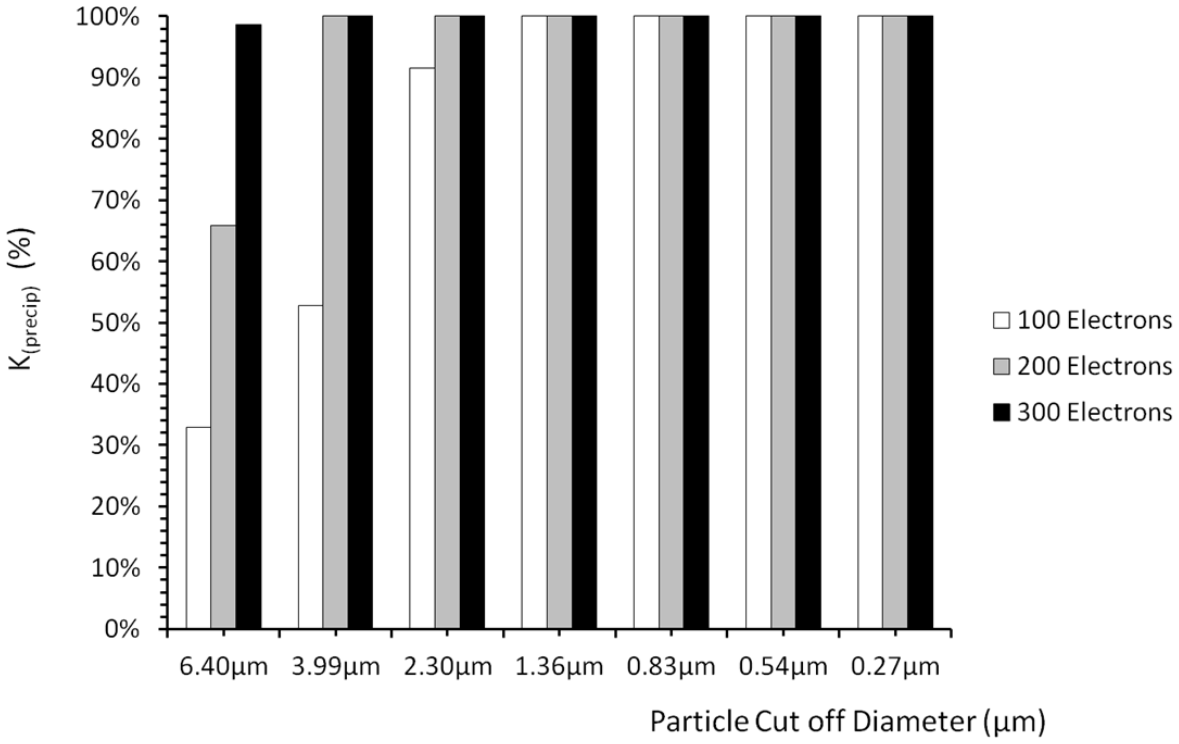
100%
90%
80%
70%
60%
50%
40%
30%
20%
10%
0%
$K_{(precip)}$ (%)
6.40µm
3.99µm
2.30µm
1.36µm
0.83µm
0.54µm
0.27µm
Particle Cut off Diameter (µm)
100 Electrons
200 Electrons
300 Electrons

Figure 3

A

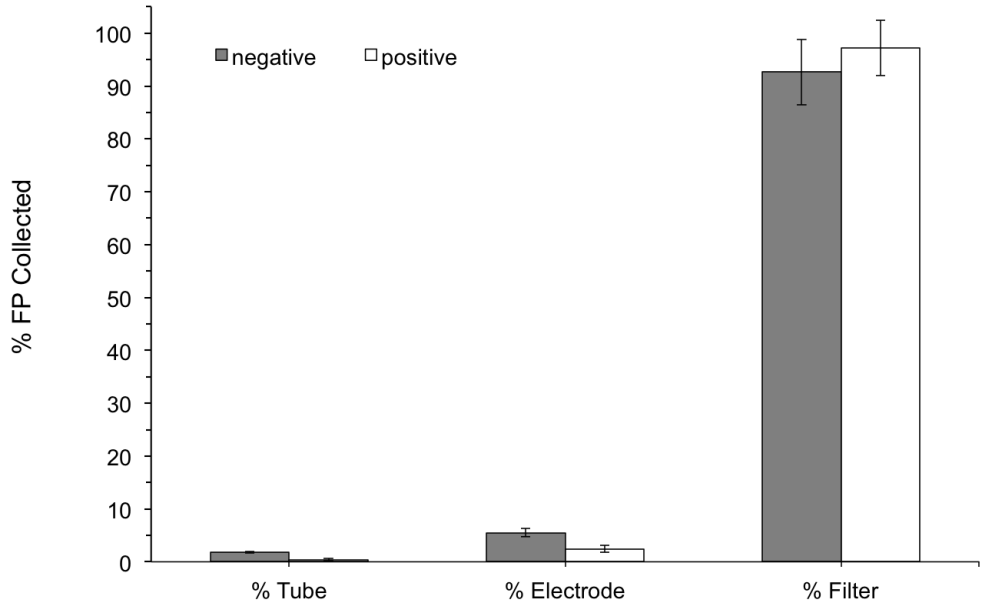
negative
positive
% FP Collected
100
90
80
70
60
50
40
30
20
10
0
% Tube
% Electrode
% Filter

B

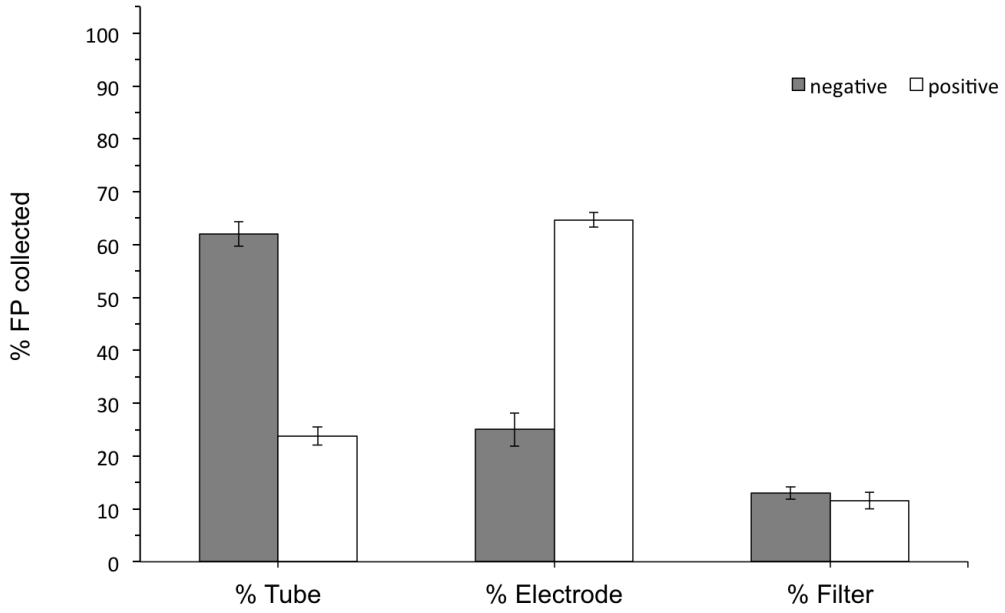
negative
positive
% FP collected
100
90
80
70
60
50
40
30
20
10
0
% Tube
% Electrode
% Filter

Figure 4

A

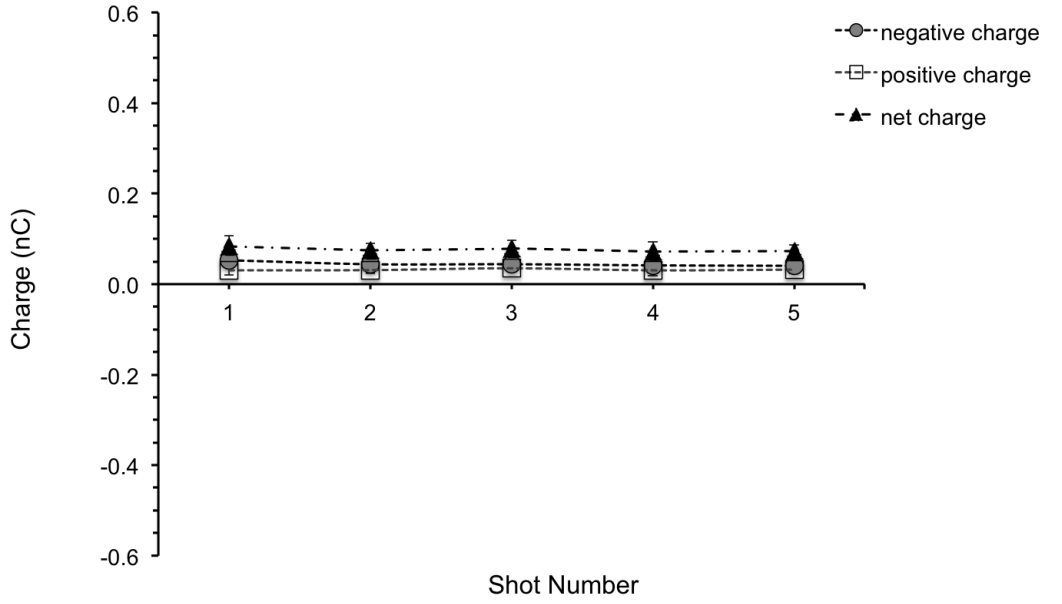
negative charge
positive charge
net charge
Charge (nC)
0.6
0.4
0.2
0.0
-0.2
-0.4
-0.6
1
2
3
4
5
Shot Number

B

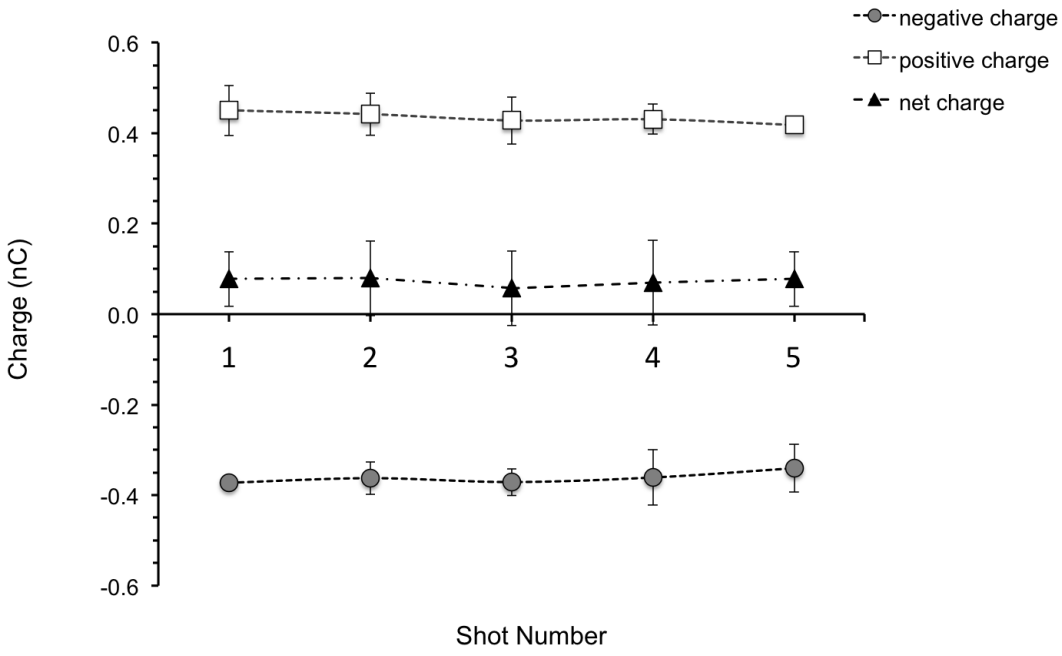
negative charge
positive charge
net charge
Charge (nC)
0.6
0.4
0.2
0.0
-0.2
-0.4
-0.6
1
2
3
4
5
Shot Number

Figure 5

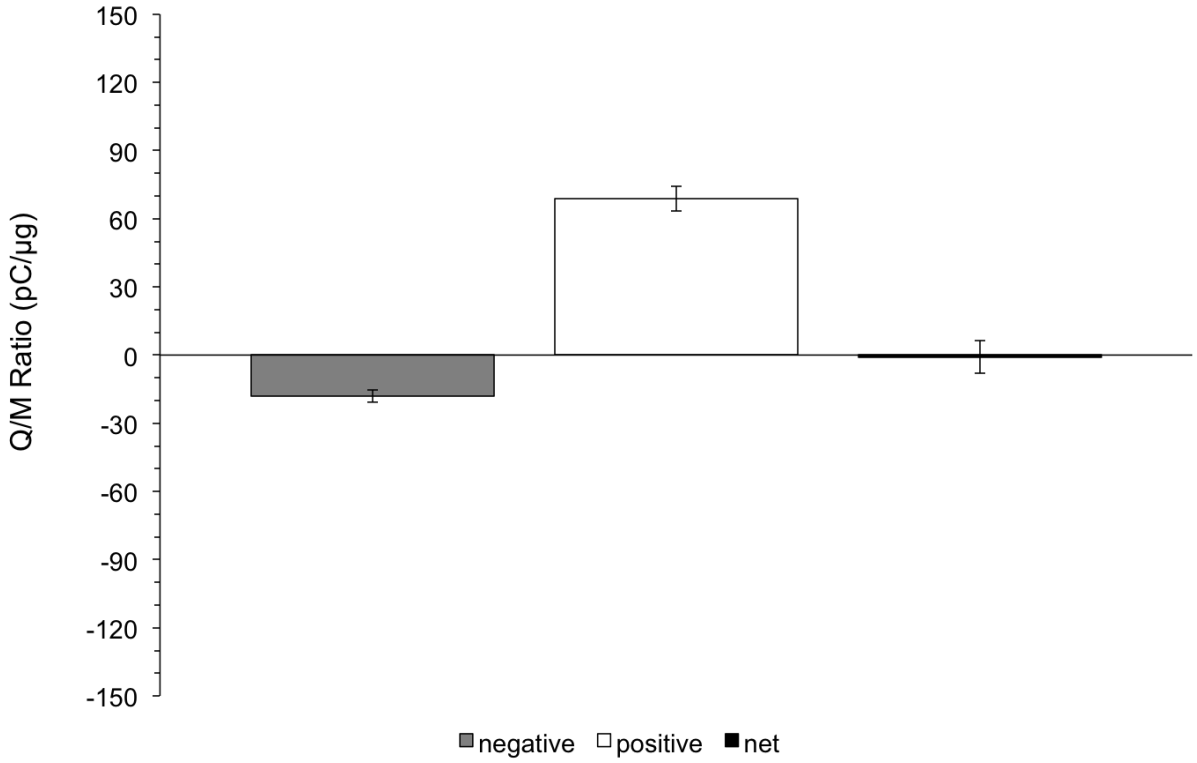
150
120
90
60
30
0
-30
-60
-90
-120
-150
Q/M Ratio (pC/µg)
negative
positive
net

Figure 6

A

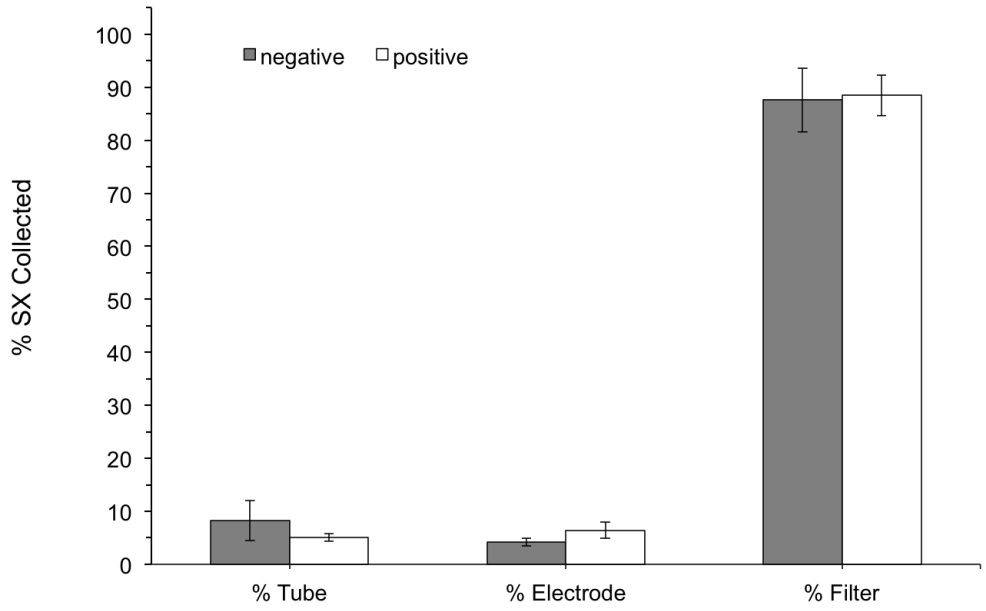
negative
positive
% SX Collected
100
90
80
70
60
50
40
30
20
10
0
% Tube
% Electrode
% Filter

B

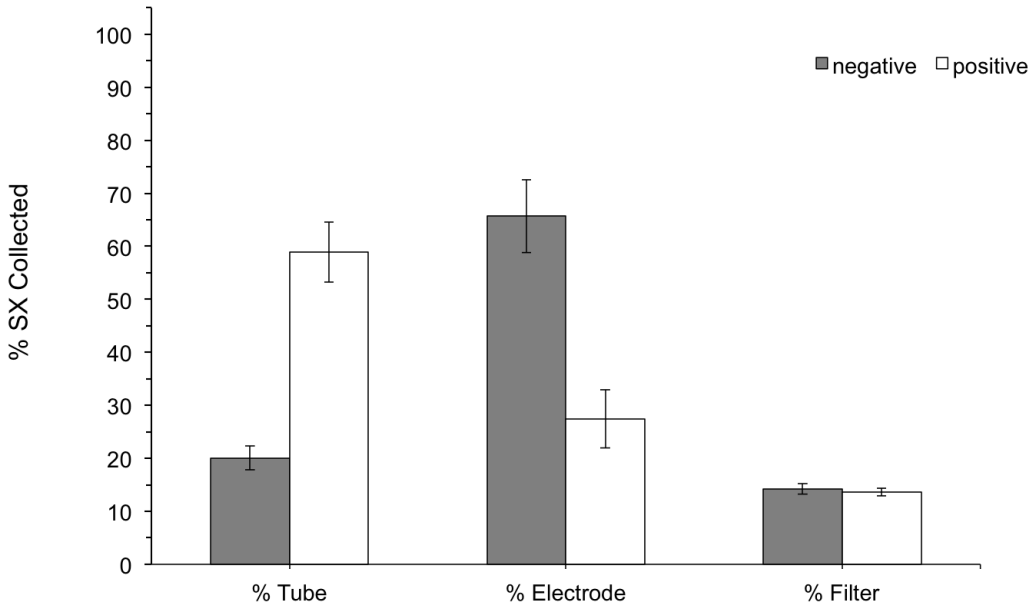
negative
positive
% SX Collected
100
90
80
70
60
50
40
30
20
10
0
% Tube
% Electrode
% Filter

Figure 7

A

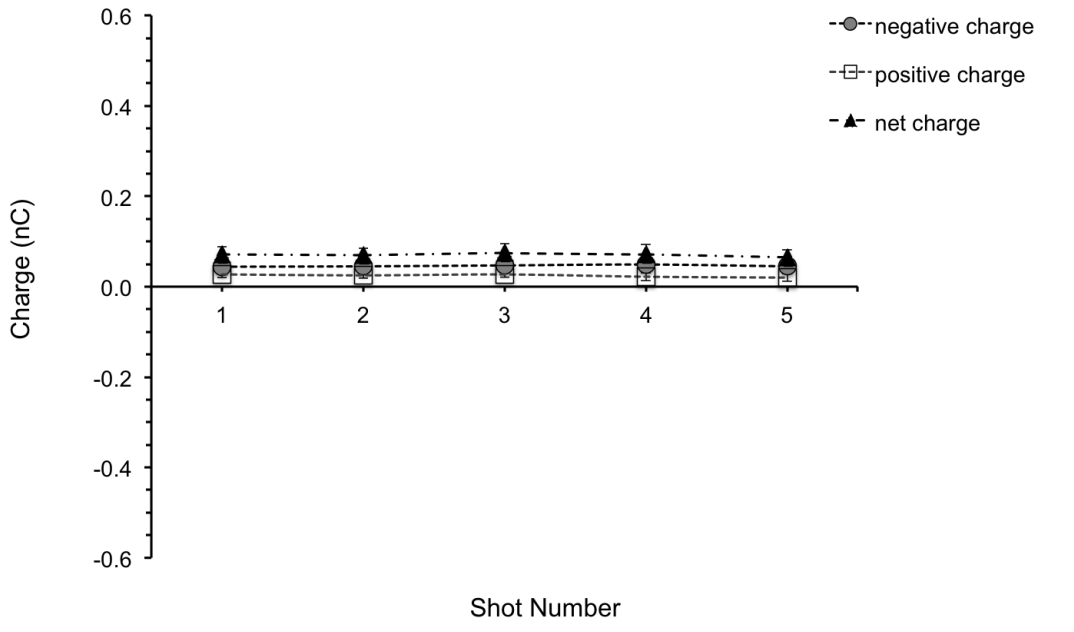
0.6
0.4
0.2
0.0
-0.2
-0.4
-0.6
Charge (nC)
1
2
3
4
5
Shot Number
negative charge
positive charge
net charge

B

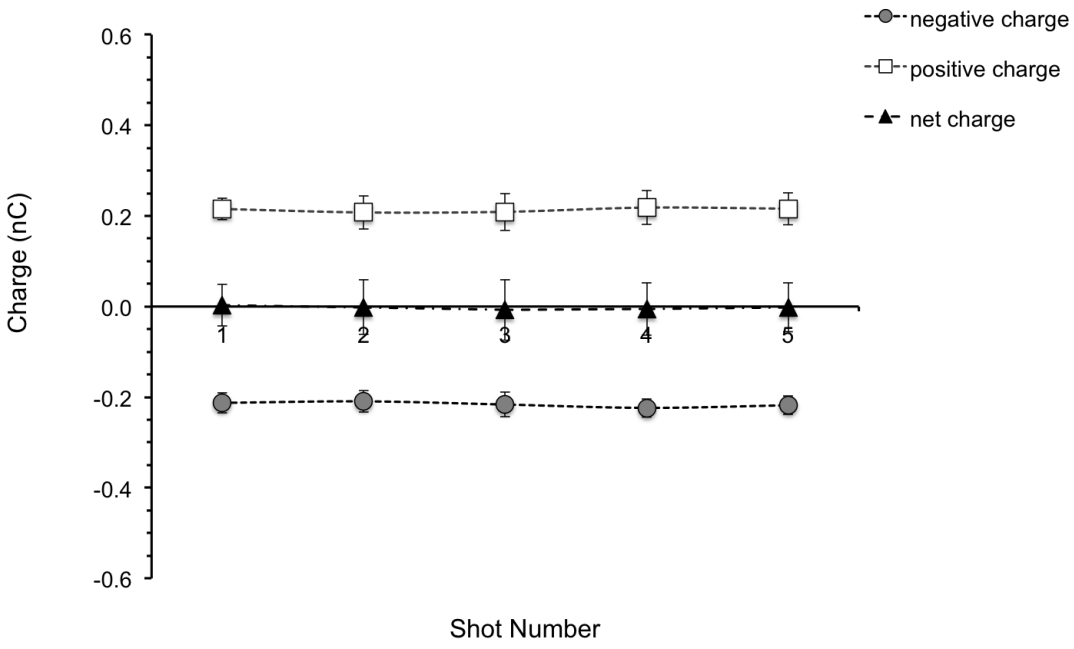
0.6
0.4
0.2
0.0
-0.2
-0.4
-0.6
Charge (nC)
1
2
3
4
5
Shot Number
negative charge
positive charge
net charge

Figure 8

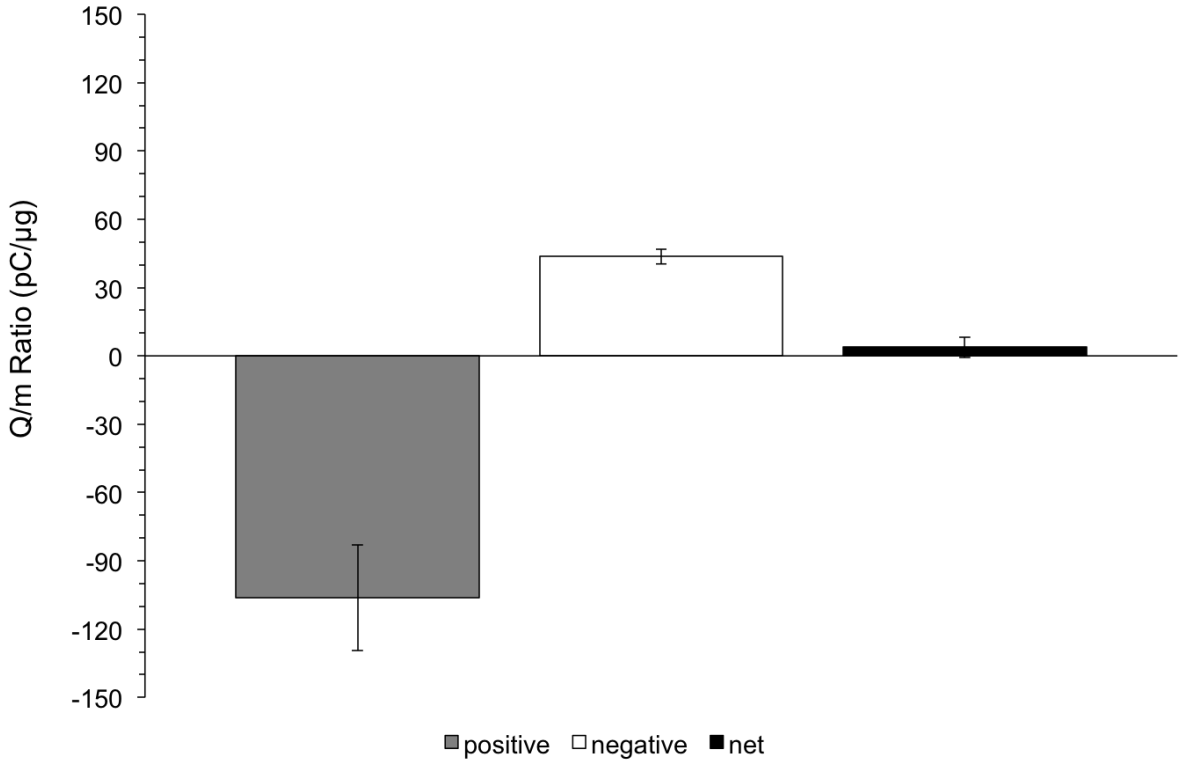
150
120
90
60
30
0
-30
-60
-90
-120
-150
Q/m Ratio (pC/µg)
positive
negative
net

Figure 9

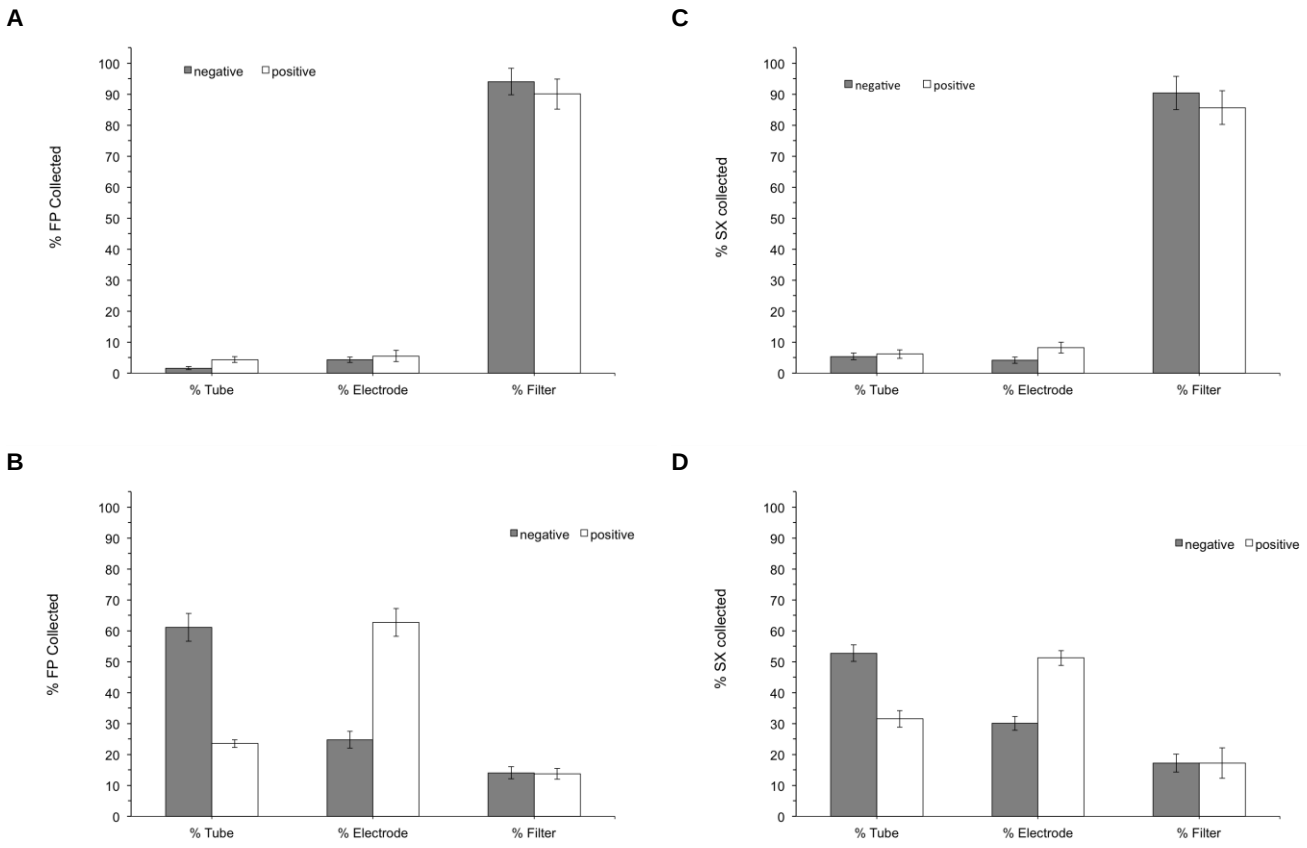
A
negative
positive
% FP Collected
% Tube
% Electrode
% Filter
C
% SX collected
B
D

Figure 10

A

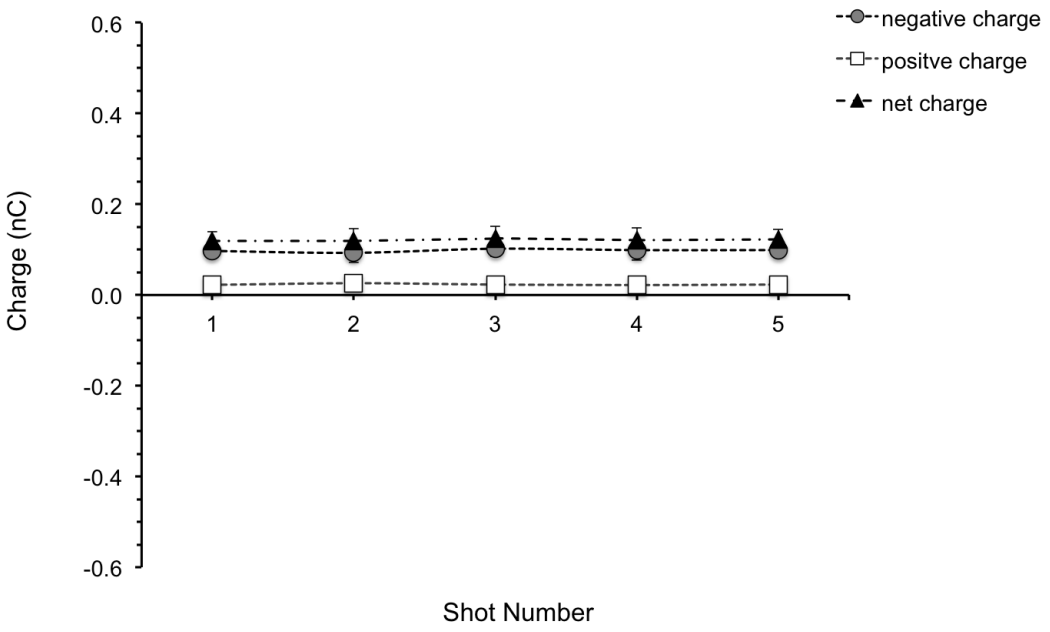
negative charge
positve charge
net charge
0.6
0.4
0.2
0.0
-0.2
-0.4
-0.6
Charge (nC)
1
2
3
4
5
Shot Number

B

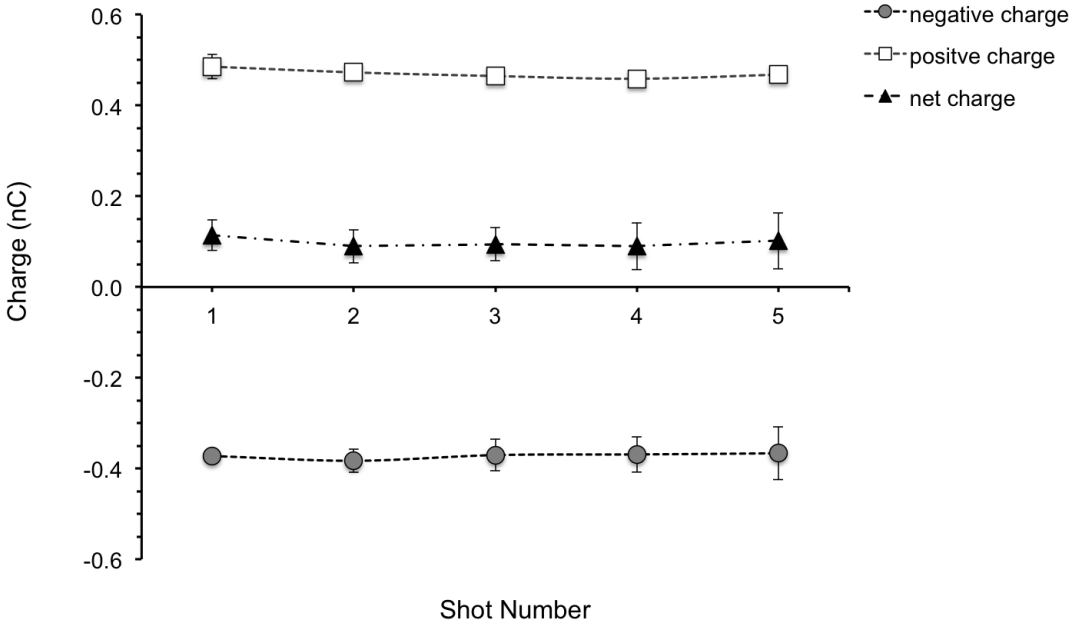
negative charge
positve charge
net charge
0.6
0.4
0.2
0.0
-0.2
-0.4
-0.6
Charge (nC)
1
2
3
4
5
Shot Number

Figure 11

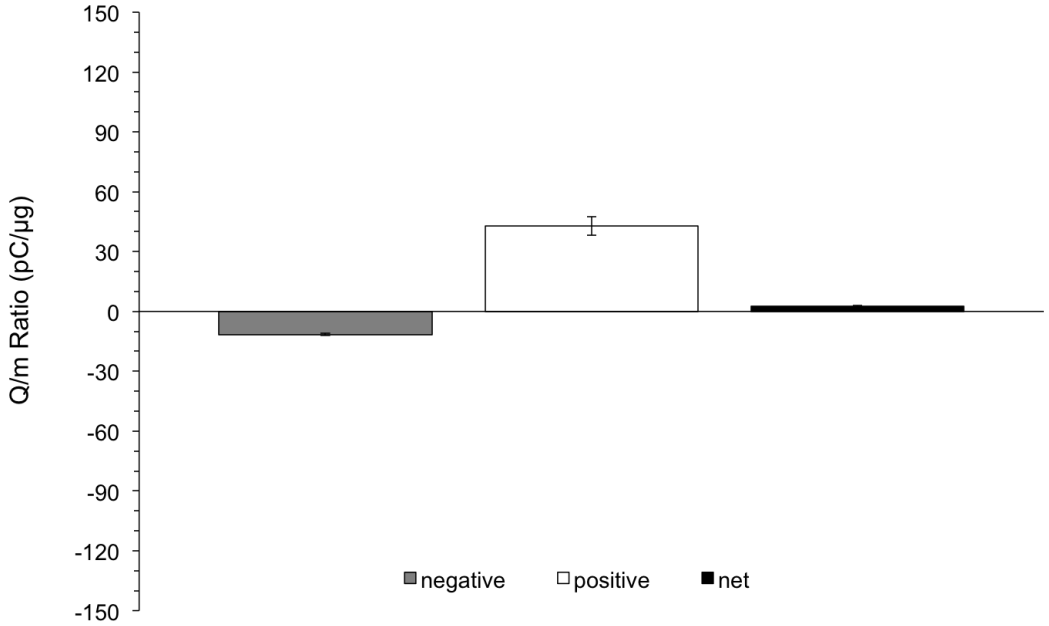
150
120
90
60
30
0
-30
-60
-90
-120
-150
Q/m Ratio (pC/µg)
negative
positive
net